Sound focusing in rooms. II. The spatio-temporal inverse filter

Sylvain Yon, Mickaël Tanter,[a] and Mathias Fink
Laboratoire Ondes et Acoustique, Université Paris VII/ESPCI, CNRS UMR 7587, 10 rue Vauquelin, 75231 Paris, Cedex 05, France

(Received 31 December 2003; revised 12 September 2003; accepted 20 September 2003)

The potential of time reversal processing for room acoustics has been extensively investigated in the companion of this paper [J. Acoust. Soc. Am. **113**(3), 1533–1543 (2003)]. In particular, a simple implementation of a loudspeaker time reversal antenna able to take advantage of the multiple reflections in reverberating rooms demonstrates its potential for audible range acoustics while improving focusing both in space and time. However, loss of information (e.g., sound absorption in walls or nonequalized bandwidths of the loudspeakers) during a time reversal experiment degrades the quality of time reversal focusing. In this paper, a more sophisticated technique called spatio-temporal inverse filtering is investigated that achieves time and space deconvolution of the propagation operator between the loudspeakers antenna and a set of microphones embedded inside the insonified volume. Theoretical and experimental comparisons between time reversal and inverse filter focusing are presented. Finally, advantages and limitations of both focusing approaches are highlighted. © *2003 Acoustical Society of America.* [DOI: 10.1121/1.1628247]

PACS numbers: 43.20.El, 43.60.Gk, 43.38.Hz [RLW] Pages: 3044–3052

I. INTRODUCTION

One of today's most challenging applications in room acoustics is the ability to control or focus the sound field in a predefined area of the propagation environment. Ideally, this sound control should be achieved with loudspeakers and microphones not necessarily located in the vicinity of the region of interest. This situation is common to various cases such as noise attenuation, compensation of room acoustic characteristics, or immersion in virtual sound environments (i.e., auralization).

This problem of sound control has been widely studied in terms of signal processing. Indeed, the propagation in a room between the set of emitting loudspeakers and the set of control points[1] can be assimilated to a multi-dimensional filter. One solution is then to obtain an inverse for this multi-dimensional filter and use it as a set of filters for emission.[2–4] From this ''signal processing'' point of view, the propagation in the medium is considered as a ''black box.'' From another more ''physical'' point of view, the spatial and temporal control of sound can be linked to the problem of focusing the acoustical energy on one (and possibly many) focal points.

In the companion paperd,[5] it has been shown that a technique such as time reversal could be very useful in such a context. Time reversal[6] provides an elegant way to focus acoustical energy spatially and temporally, even in complicated environments such as strongly reverberating rooms. Time reversal consists in using the time-reversed version of the Green's function associated with the desired focal point as a filter during emission. Thus, time reversal provides both spatial[7] and temporal[8] adaptive matched filtering of the medium. In some applications, this adaptive matched filter is equivalent to an inverse filter of the propagation medium. However, loss of information can appear during propagation (e.g., absorption losses, diffraction outside the recording surface,...). These information losses break the equivalence between a matched filter (time reversal) and an inverse filter of the propagation.[7,9] Indeed, this irreversible loss breaks the time reversal invariance and, consequently, time reversal does not ensure an optimal focusing.

In the context of audible range acoustics, it is interesting to compare these two different approaches (matched filtering and inverse filtering) of sound control. In order to study more specifically the problem in terms of propagation, we will introduce a spatio-temporal inverse filtering technique slightly different from the one proposed by Kirkeby *et al.*[3] This technique uses a singular value decomposition of the propagation operator, and has been proposed and studied as an adaptive focusing technique for a complex propagation environment by Tanter *et al.*[7,9] in the context of medical ultrasound. In particular, this approach allows one to link the singular value decomposition of the propagation operator to the plane wave decomposition of the wavefield.[9]

This paper is divided into three main sections: First, a matrix formalism is introduced to describe the slight differences between time reversal and inverse filtering. Next, experimental results are presented for the problem of focusing sound inside a room. These experiments show to what extent the quality of focusing is directly linked to the quality of reverberation in the room. In particular, it is shown that these sound control techniques can be used even if propagation conditions are very complex. For example, focusing can be achieved when loudspeakers are in one room and the area to control is in another one. Finally, we experimentally demonstrate how the multiple reverberations of sound in walls can be used to achieve a super-resolution focusing of sound. Such a super-resolution effect has already been previously explained by our group for multiple scattering and strongly reverberating media[10–12] and numerically studied by

[a]Author to whom correspondence should be addressed. Electronic mail: michael.tanter@espci.fr

Blomgren *et al.*[13] We now consider its application to the domain of audible range acoustics.

II. INVERSE FILTER AND TIME REVERSAL

A. The propagation operator $\{h_{mj}\}(t)$

We define the linear operator relating the J elements of the transducer array to the set of M control points located in the medium. We define an impulse response $h_{mj}(t)$ for each couple (m,j) comprising a control point and a loudspeaker. This impulse response $h_{mj}(t)$ is the signal received at the mth control point when a temporal delta function is applied on the jth loudspeaker. This response includes all the propagation effects in the considered medium, as well as the acousto-electric responses of the loudspeakers and microphones. This set of $M \times J$ temporal functions characterizes the *propagation operator* describing both the propagation environment and the transducer configuration.

Let $e_j(t)$, $1 \leqslant j \leqslant J$, be the J input signals for the loudspeakers. The output signals $f_m(t)$, $1 \leqslant m \leqslant M$, received by each microphone are

$$f_m(t) = \sum_{j=1}^{J} h_{mj}(t) \underset{t}{*} e_j(t), \quad 1 \leqslant m \leqslant M, \tag{1}$$

where $\underset{t}{*}$ is the temporal convolution operator. A temporal Fourier transform leads to the relation

$$\mathbf{F}(\omega) = \mathbf{H}(\omega)\mathbf{E}(\omega) \quad \forall \omega, \tag{2}$$

where $\mathbf{E}(\omega) = \{E_j(\omega)\}_{1 \leqslant j \leqslant J}$ is the column vector of the Fourier transform of the transmitted signals and $\mathbf{F}(\omega) = \{F_m(\omega)\}_{1 \leqslant m \leqslant M}$ is the column vector of the Fourier transform of the received signals. The transfer matrix $\mathbf{H}(\omega) = \{H_{mj}(\omega)\}_{1 \leqslant m \leqslant M, 1 \leqslant j \leqslant J}$ is the temporal Fourier transform of $\{\mathbf{h_{mj}}\}(t)$.

B. Time reversal and inverse filtering

As explained in the Introduction, the time reversal focusing technique consists in playing backwards the signals received at each loudspeaker location after emission of a single impulse at the desired focal spot location. Thus, the emitted signals can be written

$$e_j(t) = h_{m_0 j}(-t) = \{h_{mj}\}(-t) \underset{t}{*} \boldsymbol{\delta}_{m_0}(t), \tag{3}$$

where $\boldsymbol{\delta}_{m_0}(t)$ is null everywhere, except for $m = m_0$ and $t = 0$ [$\boldsymbol{\delta}_{m_0}(t)$ is a temporal and spatial delta function distribution]. After propagation in the medium, the signals received at the control points can be written

$$\mathbf{f}_m(t) = \left\{ \sum_{j=1}^{J} \mathbf{h}_{mj}(t) \underset{t}{*} \mathbf{h}_{mj}(-t) \right\} \underset{t}{*} \boldsymbol{\delta}_{m_0}(t). \tag{4}$$

In the frequency domain, Eq. (4) can be written for each frequency component ω:

$$\mathbf{F}(\omega) = \mathbf{H}(\omega)\mathbf{H}^{\dagger}(\omega)\Delta_{m_0}, \tag{5}$$

where † denotes the transpose conjugate operation, and $\Delta_{m_0} = [0 \cdots 010 \cdots 0]^{\dagger}$. Thus, the signals $\mathbf{F}(\omega)$ are linked to the description function Δ_{m_0} and the operator $\mathbf{HH}^{\dagger}$ known in the literature as the time reversal operator.[14]

The inverse filtering technique is based on an approximation of the inverse of $\mathbf{H}$. The problem of the inversion of the matrix propagator $\mathbf{H}$ is of course ill-conditioned. First, noise introduced during the acquisition of $\mathbf{H}$ would produce very large errors in the reconstructed results. However, even if the measurement was perfect, $\mathbf{H}$ is not necessarily invertible. Many techniques for the regularization of this problem have been described:[3] the regularization is achieved here using the singular value decomposition technique: $\mathbf{H}$ can be decomposed as

$$\mathbf{H} = \mathbf{UDV}^{\dagger}, \tag{6}$$

where $\mathbf{D}$ is a diagonal matrix containing the singular values of $\mathbf{H}$. The matrix inversion is only applied to the physically relevant singular vectors of $\mathbf{H}$, which gives a noise filtered approximation of $\mathbf{H}^{-1}$:

$$\hat{\mathbf{H}}^{-1} = \mathbf{V}\hat{\mathbf{D}}^{-1}\mathbf{U}^{\dagger} = \mathbf{V} \begin{bmatrix} \lambda_1^{-1} & 0 & \cdots & \cdots & 0 \\ 0 & \ddots & 0 & & \vdots \\ \vdots & 0 & \lambda_{N(\omega)}^{-1} & & \vdots \\ \vdots & & & 0 & \vdots \\ 0 & \cdots & \cdots & \cdots & 0 \end{bmatrix} \mathbf{U}^{\dagger}, \tag{7}$$

where N is the number of physically relevant singular values at the frequency ω. Thus, for a given field distribution objective $F_0(\omega)$, we can calculate the set of emission signals $E(\omega)$ that should give rise to $F_0(\omega)$ after propagation in the medium. After emission of $E(\omega)$ by the loudspeakers and propagation in the medium, the field obtained at the set of control points is

$$F_{pr}(\omega) = \mathbf{H}\hat{\mathbf{H}}^{-1}F_0(\omega). \tag{8}$$

It appears from Eqs. (7) and (8) that accurate reconstruction of the target field depends significantly on the number of relevant singular values. For a given frequency, the number of relevant singular values can be predicted for simple cases from the geometry of the problem. As explained by Tanter *et al.*,[7] in the case of free space propagation between two linear parallel arrays, this number N is given by the relation

$$N = 2\frac{L}{\lambda}\sin\left(\tan^{-1}\frac{D}{2F}\right), \tag{9}$$

where D and L are the width of the emitting and receiving arrays, respectively, and F is the distance between the two antennas. The number of degrees of freedom for the propagation operator, N, can be seen as the number of independent focal spots (lateral width $\sim \lambda F/D$) that can be created at the control points aperture L. It also represents the capacity given by the propagation medium and the geometrical disposition of the antenna to recreate a complicated sound field at these control points: if the projection of this desired field on the physically relevant singular vectors does not result in significant loss of information, the system will be able to create the desired sound field with a good accuracy. Thus, projecting on the main singular vectors the wavefield distri-

bution that we would like to achieve at the control points is a good way to predict the wavefield that will be obtained experimentally. Equation (9) relates N to the parameters of the problem in a free space environment. In the case of reverberating rooms, previous works[5,10] indicate that an increase in the number of degrees of freedom due to the increase of the emitting antenna apparent diameter leads to an improvement of the focusing pattern obtained by time reversal. The same result will be presented in this paper for room acoustics.

It has been shown in ultrasound that time reversal tends to achieve an inverse filter of the propagation when no loss of information (e.g., absorption effects, diffraction of the wavefield outside the array aperture, limited spatial directivity and bandwidth of the emitters and receivers) appear during the first step of a time reversal experiment.[7,9] In our case, such information losses are of particular interest as, for example, sound absorption occurs in walls. In addition, even high end loudspeakers have irregular transfer functions, leading to a degradation of the bandwidth that is not compensated and even amplified by time reversal techniques. Thus, in audible range acoustics, there should be some differences between the focusing quality obtained by time reversal and the spatio-temporal inverse filter. By introducing a time and space deconvolution process, the spatio-temporal inverse filtering process provides a way to compensate partially, sometimes completely, for electronics limitations but also spatial setup limitations. In Sec. III, experimental comparisons between time reversal and inverse filtering illustrate this purpose.

III. EXPERIMENTAL RESULTS IN ROOMS

A. Experimental setup

The first series of experiments have been carried out in an empty room with reverberant walls, floor and ceiling. The considered room dimensions are $5.75\times3.45\times3$ m^3 and the Sabine reverberation time (the standard reverberation time has been defined as the time for the sound to die away to a level 60 dB below its original level) is quite long due to the absence of acoustical energy absorbers such as furniture: $T_{60}=1{,}56$ s. In order to study the propagation operator, an antenna made of 16 Audax AX34 loudspeakers is placed near one of the walls (see Fig. 1). The set of control points consists of 25 points located along an axis parallel to the loudspeaker antenna. The impulse responses are acquired successively using a microphone translated to each control point position. The first step of each experiment consists in acquiring the propagation operator $h_{mj}(t)$. In order to obtain a good signal-to-noise ratio, the process is as follows: first, the microphone is placed in position j; then, a chirp signal is emitted from loudspeaker m, over the usable frequency range of the system (400–4000 Hz). The signal measured with the microphone is then correlated with the original chirp in order to obtain the impulse response between loudspeaker m and control point j.

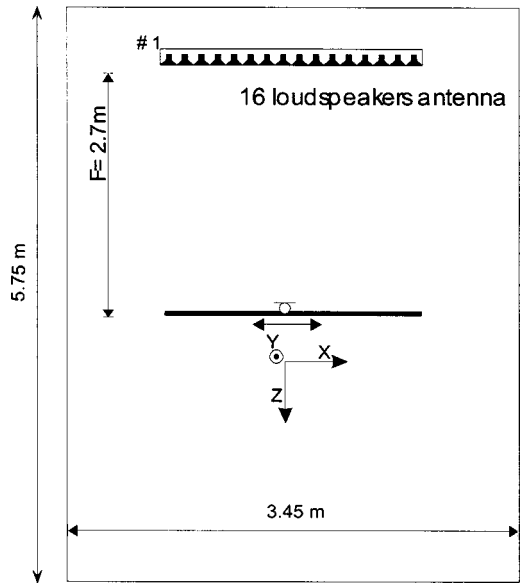

FIG. 1. Setup for the experiments in a reverberating room.

B. The propagation operator

The propagation operator corresponding to the setup described above is first acquired: To measure the impulse response $h_{mj}(t)$, the mth loudspeaker emits a linear chirp in the band 400 Hz to 4 kHz. The corresponding signals are then acquired at each of the J control points. Signals are then correlated with the initial chirp to obtain $h_{mj}(t)$ for each control point. This process is then iterated for each loudspeaker.

After adequate windowing and filtering, the frequency domain representation of propagation operator $H_{mj}(f)$ is obtained. In order to be able to invert matrix $\mathbf{H}$ for each frequency, we must identify which part of $\mathbf{H}$ is related to experimental noise, and which part is related to relevant propagation information. As explained above, only singular vectors corresponding to high singular values should be used during inversion. For this reason, it is important to be able to determine a simple method for differentiating the physically relevant singular values from the ones corresponding to noise. Such a differentiation is made easy by studying the distribution of the singular values plotted in decreasing order as a function of frequency (referred to as the singular value space). Figure 2 gives an example of this representation.

As explained previously, the number of relevant singular values of the propagation operator corresponds to the number of available degrees of freedom for the reconstruction of the desired field. In Fig. 2, the singular value space is calculated in two configurations: in the first configuration, the direct wavefront is detected in the temporal propagation operator, and this single wavefront is used to calculate the singular value space. In others words, no reverberations are taken into account in the free space propagation operator. This is an easy way to obtain a good approximation of the propagation in free space, with the same configuration for emitting transducers and control points. Figure 2(a) presents the singular values distribution of this free space propagation operator. In the second configuration, the complete propagation operator (direct propagation+reverberations) is taken into account

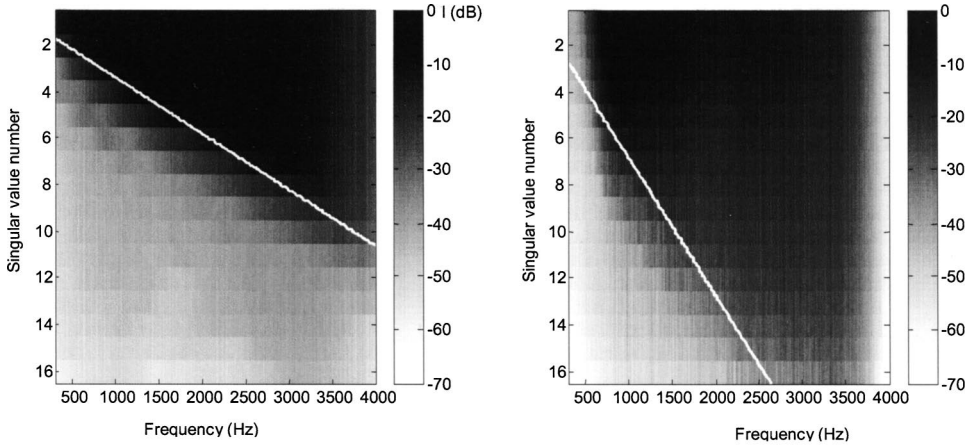

FIG. 2. Singular values space (a) for the propagation operator in free space (after cancellation of the reverberations) and (b) in the reverberating room.

during the singular value decomposition. The singular value space in Fig. 2(b) corresponds to the entire propagation operator when propagation occurs in the reverberant room. As one can notice by comparing Figs. 2(a) and (b), the fact that propagation occurs in a reverberating environment strongly increases the number of degrees of freedom available for each frequency.

This increase of the number of freedom degrees can be explained from a ''diffraction'' point of view: in the case of free space propagation, the finite aperture of the emitting antenna limits the number of independent focal spots (with a lateral resolution $\lambda F/D$) that can be created in the control points aperture L with respect to Eq. (9). Moreover, according to Eq. (9), N should increase linearly with frequency:

$$N = 2f\frac{L}{c}\sin\left(\tan^{-1}\frac{D}{2F}\right), \tag{10}$$

where c is the sound speed. This linear frequency dependence on N is clearly found in the singular value space of the experimental propagation operator in Fig. 2(a). The white line in Fig. 2(a) corresponds to the theoretical Eq. (10) and clearly fits the experimental separation between noise space and singular value space. In the case of a reverberating room, the numerous reflections against the walls create a set of virtual sources corresponding to the mirror images of real loudspeakers in regards to each wall. An observer located at the focal point does not only hear the real loudspeakers but also their images through the wall mirrors, as shown in Fig. 3. Thus, reflections on boundaries allow one to create a virtually infinite array of emitting transducers in every direction. In this case, the focal spot size should be only limited by the classical diffraction minimal width $\lambda/2$. Consequently, the number of degrees of freedom of the propagation operator should reach its maximum value $N = 2L/\lambda = 2fL/c$. Of course, in these experiments, walls are not perfectly reflecting and the amplitude of signals decreases progressively with the number of walls reflections. However, as it results in a slight and progressive loss of amplitude, only the relative weight of each eigenvalue is affected at a given frequency. Thus, Eq. (10) remains valid even in experimental conditions as it deals with the total number of relevant eigenvalues at a given frequency. The theoretical line $N(f) = 2fL/c$ is plotted in Fig. 2(b) and shows a good agreement between the theoretical description and real measurements. Moreover, it confirms that we should be able to create spots of $\lambda/2$ diameter at the set of control points by using correctly the walls reverberations.

The results given in Fig. 4 provide confirmation of the above analysis. The spatial frequency spectrum of the different singular vectors is plotted for $f_0 = 1500$ Hz. The dashed lines separate the singular vectors corresponding to noise from the ones corresponding to physically relevant data. It appears that the spatial frequency bandwidth of physically relevant singular vectors is larger in the case of reverberant rooms, which includes the higher spatial frequencies corresponding to plane wave angles of arrival that cannot be attained when considering only the emitter array in free space. Thus, working in a perfectly reverberant environment allows us to reconstruct a sound field with a large spatial frequency spectrum. In practical applications, it means that such an environment makes it possible to simulate a sound field with any direction of arrival regardless of the positions of the emitters. Of course, this description corresponds to a case where no attenuation occurs during the reflections. In practical systems, however, attenuation implies that the spatial frequencies corresponding to a significant number of reflections

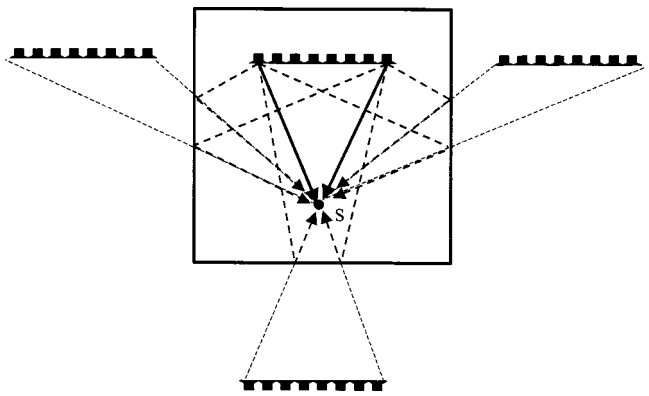

FIG. 3. Principle of the mirror images: an observer S located at the focal point does not only hear the real loudspeakers but also their images through the wall mirrors.

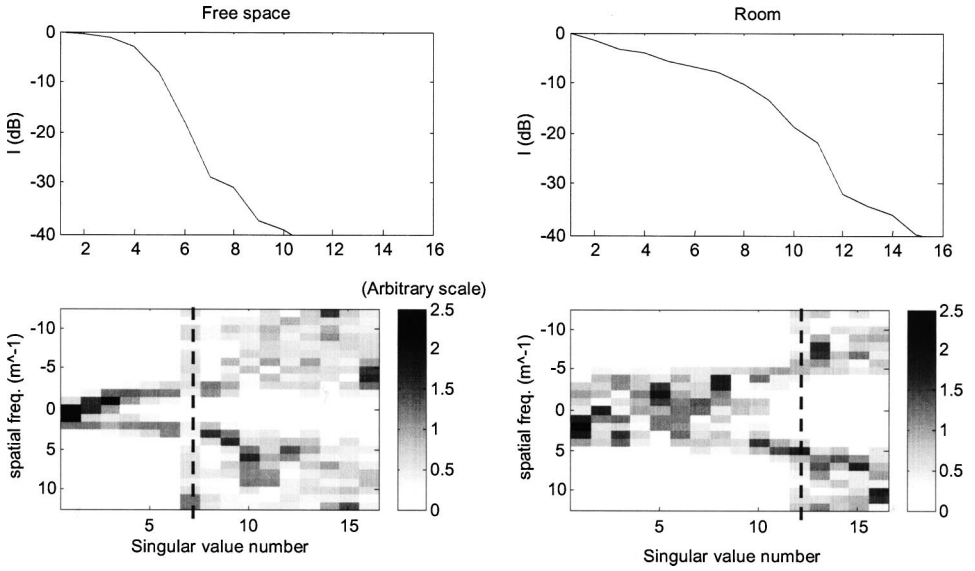

FIG. 4. Singular values weights and corresponding spatial Fourier transform in the emitting plane of the singular vectors of the propagation matrix for the frequency $f_0 = 1500$ Hz.

are sometimes not available. In that case, the spatial positions of the emitters play an important role.

To be able to invert the propagation operator, a separation must be established between the physically relevant part and the noise part of the propagation operator. This separation is easily established from the results presented in Figs. 2 and 4. Indeed, there is a brutal variation in the intensity of the singular values from 0–10 dB to less than −30 dB and this variation corresponds to the appearance of noise in the singular vectors. Thus, in our series of experiments, a limit value of −25 dB will be used for considering that singular values are physically relevant, and may be used in the inversion.

C. Focusing and sound control capacity

Once the propagation operator has been acquired and a good approximation of its inverse form has been calculated as explained above, emission filters $e_j(t)$ are easily calculated for a given field distribution objective $f_{m0}(t)$. Though the desired field can be whatever is needed, our initial interest is to obtain a single focal spot, since any field distribution can be deducted from this simple one.

Through the inverse filtering process and the backpropagation operation [Eq. (8)], we obtain a least mean squares approximation of the desired sound field $f_{m0}(t)$. No specific condition is imposed by the algorithm on this sound field, but physical characteristics of the propagation medium and of the electronic emission/reception system have to be taken into account. Thus, $f_{m0}(t)$ must be chosen according to those characteristics, otherwise the algorithm will use too much energy in trying to recreate a nonphysical field, resulting in an increased noise level. To take into account these conditions for the case of propagation in the room, two points must be respected: (1) The frequency content of the sound field must be included in the bandwidth of the electronic system and (2) the focal spot width cannot be less than $\lambda/2$, where λ is the wavelength corresponding to the minimal frequency in the desired sound field.

Diagrams presented in Fig. 5 show the spatial focusing quality that can be achieved when the conditions explained above are respected. The temporal objective is chosen to be a pulsed signal of bandwidth of 1–3 kHz, and the desired focal spot width is fixed to 17 cm. We also consider the time reversal focusing which is obtained by performing a time reversal experiment with an initial signal identical to the one used as the objective for the inverse filter technique. Figure 5 clearly shows the improvement that can be achieved with inverse filtering compared to time reversal: the spatial sidelobe level is at least 5 dB lower for the spatio-temporal inverse filtering process.

Until here, we have considered a field objective consisting of 25 control points. In these conditions, the inverse filter and time reversal processing are not fairly compared: the quantity of information used to obtain the presented results is 25 times more important for the inverse filtering method. However, this inverse filtering process can also be achieved using fewer control points. This aspect is presented in Fig. 6 describing the evolution of the sidelobes level obtained with both techniques versus the bandwidth and the number of

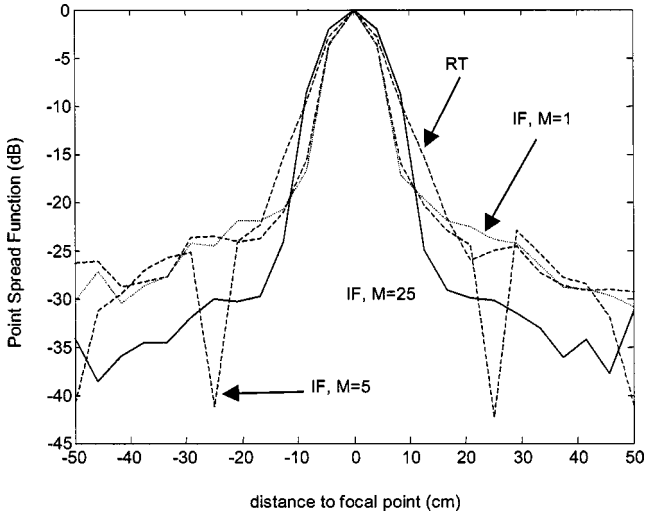

FIG. 5. Directivity patterns obtained with time reversal and inverse filtering for different numbers M of control points.

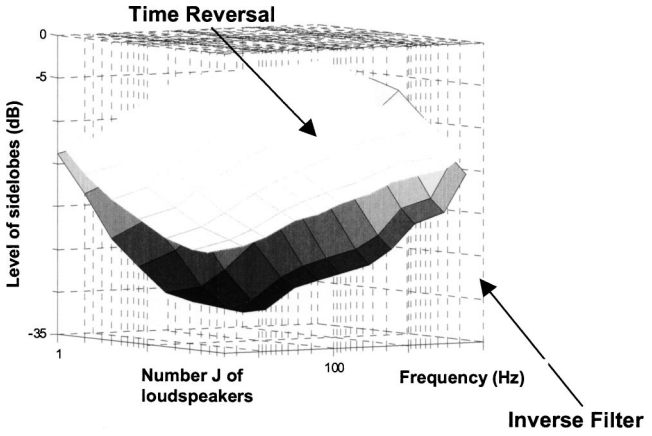

FIG. 6. Evolution of spatial sidelobe level $SL_{(dB)}$ as a function of the number of used transducers J and of the bandwidth BW, for time reversal and inverse filtering. Measurements are averaged over 16 repetitions.

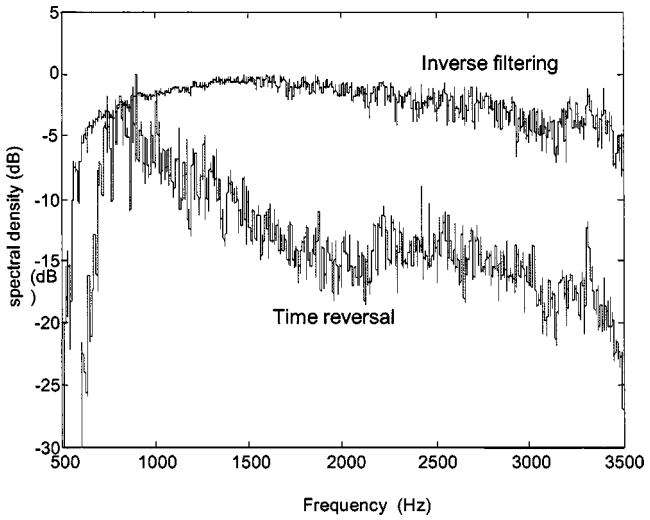

FIG. 7. Spectral content at the focal point after time reversal and inverse filtering.

transducers used. The evolution of the sidelobes level was extensively discussed for the time reversal approach in the companion of this paper[5] and we focus here on the differences between the time reversal and inverse filtering methods. Figure 6 shows that time reversal and the inverse filter give globally similar results in terms of spatial focusing for the same quantity of information. However, as it is presented in Fig. 5 for $M=5$, one of the advantages of spatio-temporal inverse filtering is that it allows us to force certain points to have a null field, with an attenuation up to -40 dB. These results correspond to signals that use the whole available frequency bandwidth and this frequency diversity is essential to obtain such spatial focusing results. Figure 6 clearly illustrates this point. It represents the level of the sidelobes obtained by time reversal and inverse filtering as a function of the used frequency bandwidth and as a function of the number J of loudspeakers emitting the time reversed or inversed signals. The improvement of the level of the sidelobes by inverse filter focusing compared to time reversal is only significant when the frequency bandwidth of the emission signal becomes important. Unfortunately, common signals such as speech are characterized by the fact that in practice only a few frequencies (corresponding to formants) are emitted. As explained in Ref. 5, such signals are quasi-monochromatic from the point of view of diffraction, and lead to similar point spread functions whatever technique is used. Thus, in terms of spatial distribution of the acoustic energy, focusing of speech (quasi-monochromatic) signals is almost identical when using the time reversal or inverse filtering methods.

However, important differences between the time reversal and inverse filtering methods occur in the time domain. As seen in Fig. 7, the frequency spectrum of the signal obtained at focus is quite different for both focusing methods. Contrary to time reversal, the inverse filter focusing technique introduces a frequency bandwidth equalization by achieving a space and time domain deconvolution. This deconvolution corrects for the non-flat amplitude response of the loudspeakers but also for the frequency dependent absorption effects occurring during propagation. One should notice in Fig. 8 that this space and time deconvolution achieved by the inverse filtering technique is not equivalent to the combination of time reversal with bandwidth equalization (in others words, a inverse filter technique with a single control point located at focus). At focus, the temporal sidelobes are almost 20 dB lower for the inverse filtering technique than for time reversal (Fig. 8). The focal signal shape obtained by inverse filtering is sharper, thus permitting attainment of a very good temporal approximation of the desired impulse signal.

D. Robustness with respect to changes in the acoustic environment

In practical systems, sound control needs to be robust, especially in the frequency domain of potential applications:

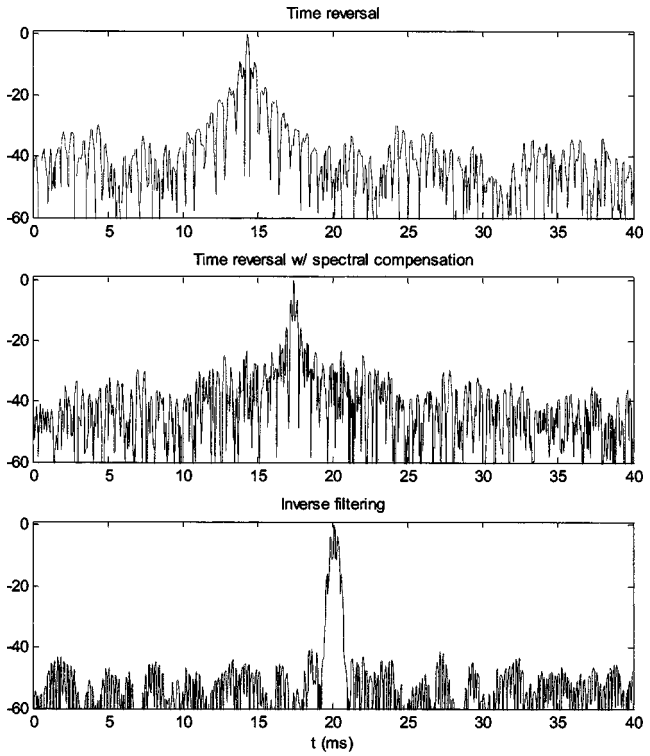

FIG. 8. Temporal sidelobes and temporal recompression observed at the focal spot, for the different techniques. The signal amplitude is presented in a dB scale.

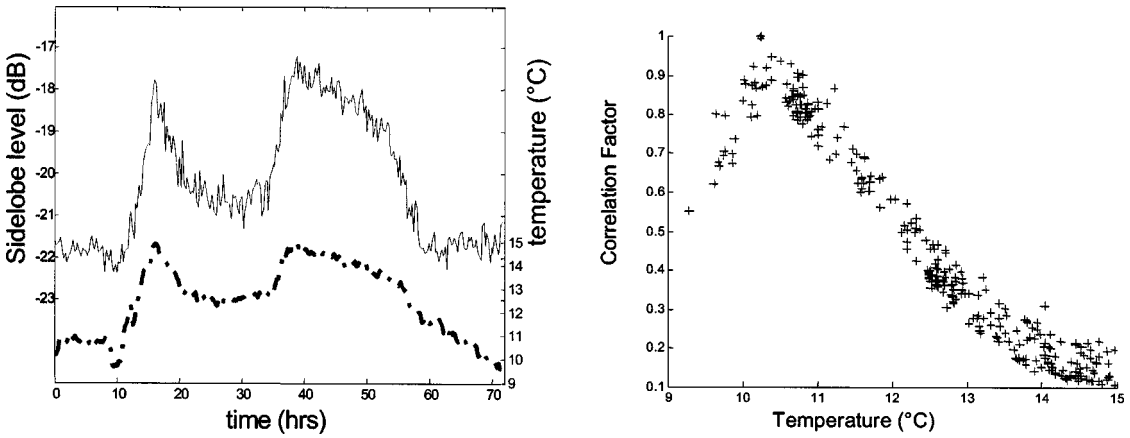

FIG. 9. Robustness of focusing versus temperature and time: initial time $t=0$ corresponds to the acquisition of the propagation operator. The solid line corresponds to the evolution of the level of the sidelobes while focusing every 15 min at the same focus location. The dashed line corresponds to the evolution of temperature operating at the same time.

sound control has to be achieved in media where objects will eventually move and where propagation conditions can vary in time. The influence of such an evolution has been measured in two ways: first, the quality of focusing was measured with different perturbations in the room, such as moving persons, or the introduction of sound absorbing objects. These tests did not show any significant variation of the focusing in terms of the spatial and temporal sidelobes level or the focal spot width.

In a second experiment, the focusing robustness regarding slow variations of the propagation medium is tested over a long time period (48 h). To study this evolution, an initial propagation operator is acquired at a time $t=0$ (room temperature $T=11\,^{\circ}\mathrm{C}$) using the technique described above. From this operator, a set of emission signals is calculated by inverse filtering for a sound field objective $f_{m0}(t)$ such as described in Fig. 5 (desired focal spot width is λ). This set is then reemitted every 15 min in order to study the evolution of the sidelobes level versus time. A preliminary experiment shows that during 48 h, no important degradation of the focusing occurs. However, the inverse filtering technique, like time reversal, is quite sensitive to changes of the medium characteristics, such as sound speed, that induce a cumulative errors during wave propagation. Figure 9 presents the results obtained when this experiment is conducted during 48 h, with variations of the temperature of the room (i.e., variations of the sound speed, $\delta c/\delta t \sim 0.6$ m.s.$^{-1}$.°C^{-1}). An interesting point is that the focusing quality described by the level of the sidelobes when focusing at a given location returns back to its initial value when temperature is equal to the temperature of the initial measurement ($T=11\,^{\circ}\mathrm{C}$). This point can be also illustrated by calculating the correlation coefficient between the initial impulse response relating one loudspeaker to the microphone located at focus and the same impulse response acquired later during the 24-h experiment. As one can notice, this correlation coefficient reaches 1 when the temperature reaches the same value as the one corresponding to the initial acquisition of the impulse response. Thus, the problem of sensitivity to sound speed variations can easily be overcome by acquiring different data banks corresponding to different temperature conditions in the room.

E. Example of sound field shaping

One of the possible applications of sound control techniques is to recreate an approximation of a desired complex sound field on all the control points. In this context, the inverse filtering technique should provide better results since a least mean square approximation is made over the whole set of control points, whereas when time reversal is used, the approximations are calculated separately for each control point.

For this reason, the inverse filtering process is expected to be much more efficient than time reversal in such a context. Figure 10(a) corresponds to the signals received in the room at the control points when loudspeaker 1 emits a short pulsed signal. As one can notice, a lot of successive reverberations are recorded at the control points after arrival of the direct path signal. Results shown in Fig. 10(b) correspond to the sound field observed at the control points in the reverberating room, when trying to recreate the effect of a virtual pulsed sound source located at the position of loudspeaker 1

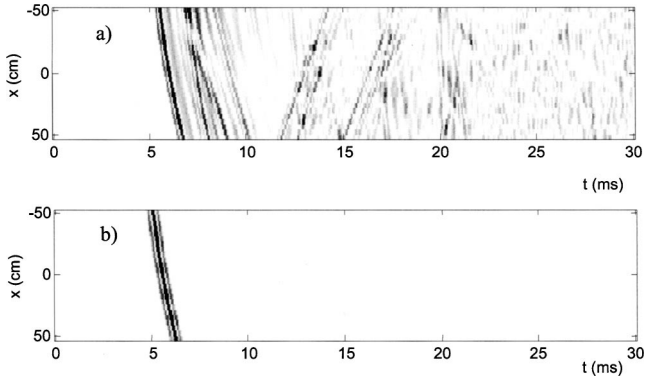

FIG. 10. Bscan representation (temporal signals received at the set of control points) (a) when loudspeaker 1 emits in the reverberating room and (b) when the inverse filter is used on the array of loudspeakers in order to recreate at the control points the virtual sound field corresponding to loudspeaker 1 emitting in free space.

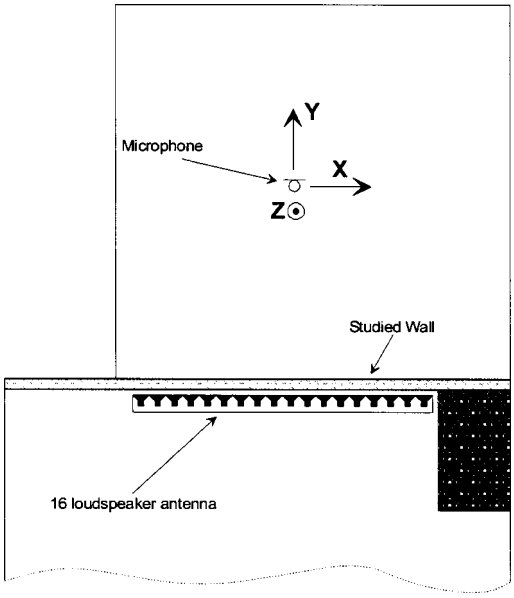

FIG. 11. Experimental setup for focusing through a wall.

(see Fig. 1) and emitting in free space. In other words, the aim is here to use the array of loudspeakers to cancel reverberations in a chosen time domain at the set of control points. As seen in Fig. 10(b), in the vicinity of the control points (vertical axis), the loudspeaker seems to emit in free space, without any reverberation. The horizontal axis corresponds to time and the signal amplitude is represented in a gray scale. Figure 10(b) is obtained with the inverse filtering technique. The reverberations induced in the room have been completely cancelled and the wavefront received at the control points seems to come from a source in a free space environment: the level of the temporal noise is more than 40 dB below the maximal amplitude received at each control points. However, when trying to recreate a similar sound field with a time reversal technique, temporal sidelobe level is here more important than those observed for a single focal spot, and the pulsed signal is wider in time. These effects, due to the fact that time reversal does not provide a way to consider the sound field as a whole, make the inverse filtering concept an interesting technique for such applications.

IV. EXPERIMENTAL RESULTS THROUGH WALLS

A. Experimental setup

In the previous section, focusing was achieved in a reverberant room. This medium is complex by itself, because of reflections and diffraction effects on every object in the room, but attenuation is not very strong. Thus, the situation corresponds to the conditions needed to achieve time reversal focusing with good precision, and differences obtained in terms of quality of focusing between the inverse filtering approach and time reversal focusing are not very important. In the companion paper,[5] it was shown that time reversal focusing could also be achieved through a wall in an experimental setup described in Fig. 11. This situation proved to be a lot more challenging for time reversal, so we try here to compare it to the optimal results by the inverse filtering technique.

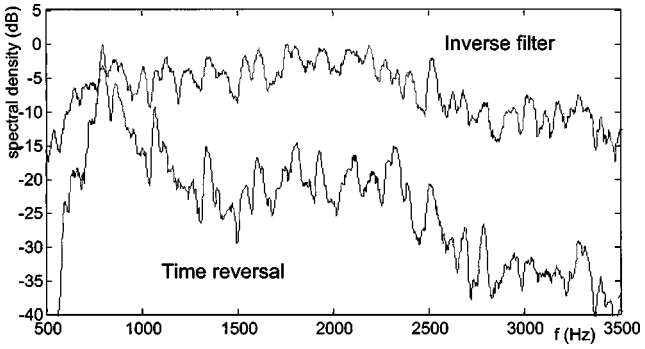

FIG. 12. Spectral content of the signal received at focus after time reversal or inverse filtering (with 25 control points).

The acoustic attenuation[15] between the central loudspeaker of the antenna and the central position of the microphone is 20 ± 3 dB. The 8-cm-thick wall by itself is made of hollow bricks and plaster. However, such a wall provides a normalized acoustic attenuation of $\sim$41 dB. Thus, the most important part of acoustical energy that manages to reach the focal point comes from ''leaks,'' probably via doors and windows, but also from lateral propagation through walls.

These complex conditions for propagation lead also to important variations of attenuation with frequency as shown in Fig. 12. So, inverse filtering could be efficient in such a case, whereas time reversal will be handicapped because it does not compensate for those variations. Experiments presented below have been achieved with exactly the same electro-acoustical and electronic devices as those used for the experiments in the room.

B. Results

As in the case of the reverberating room, relative performance of time reversal and inverse filter can be measured when trying to recreate a single focal spot, such as the ones described in Sec. III C. Theoretically, results obtained with an inverse filter should be very similar to those obtained in rooms, whereas those obtained with a time reversal technique are degraded because of attenuation during propagation. Results shown in Figs. 13 and 14 prove to be quite different from theoretical expectations.

Results obtained with an inverse filtering technique when focusing through walls prove to be as remarkable as results of Sec. III C, when considering temporal compression and noise level of obtained signals. Indeed, as it is shown in Figs. 13 and 14, inverse filtering allows one to obtain a very

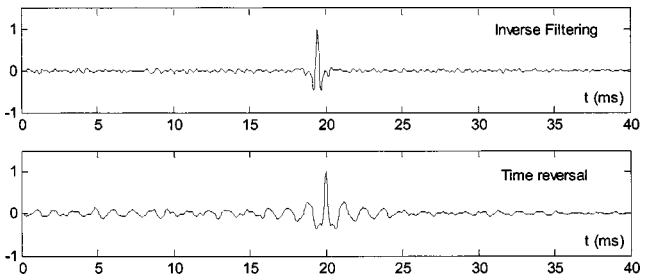

FIG. 13. Temporal recompression at the focal spot using time reversal or inverse filtering (with 25 control points).

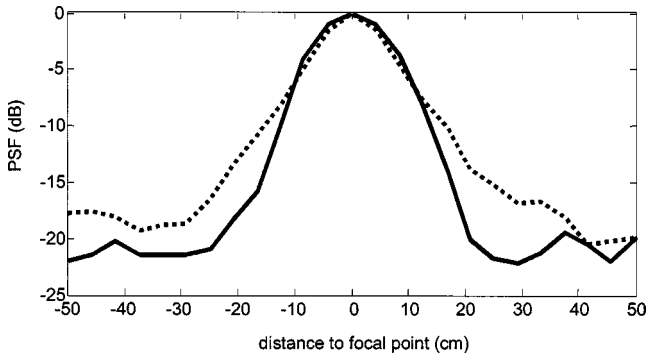

FIG. 14. Directivity patterns obtained using inverse filtering (solid line) and time reversal (dotted line) through the wall.

good temporal approximation of the desired impulsive signal at the focal spot. Specifically, the spectral density can be corrected with good accuracy over the whole bandwidth.

Figure 14 shows, however, that only a slight improvement is provided by inverse filtering compared to time reversal in terms of spatial focusing. This surprising result is only due to a technical limitation of our electronics: time reversal is a matched filter and so maximizes the energy received at the focus[7,8] whereas the inverse filter corresponds to a least mean squares approximation of the desired sound field. Thus, energy obtained at the focus for inverse filtering is lower than the one obtained with time reversal, and electronic limits of the emitting and recording devices used in the experiment were unfortunately reached. However, with a new emission/reception system providing a better dynamic range, inverse filtering should reach through the wall, similar to performances obtained in the room. Indeed, the measured sidelobe levels do not correspond to a conceptual limit, but are only due to an electronic noise limited value. Thus, while using a system with a better dynamic range, the improvement of the level of the sidelobes by inverse filtering compared to time reversal should be about 20 dB.

V. CONCLUSION

Inverse filtering is based on the knowledge of the entire propagation operator between a set of emitters and a set of control points located in the medium. For a given target sound field at the control points, this technique provides theoretically the best approximation of the field in a least mean square sense by achieving both space and time deconvolutions of the propagation operator. However, time reversal remains an interesting technique to approximate such a field because of its simplicity of implementation.

In audible range acoustics, it appears that the main advantage of inverse filter over time reversal is its capacity to compensate for the variations of the spectral densities of the transfer functions. Noise reduction at focus can reach more than 20 dB.

The spatio-temporal inverse filter should be even more adapted to complicated environments suffering propagation losses and to systems relying on low-quality electro-acoustical devices with, however, the cost of much more signal processing and the need for more amplification power.

[1] Control points correspond to a set of measurement points whose signals allow a reconstruction of the sound field in the zone of interest.

[2] V. Martin, P. Vignassa, and B. Peseux, "Numerical Vibro-acoustic modelling of aircraft for the active acoustic control of interior noise," J. Sound Vib. **176**(3), 307–332 (1994).

[3] O. Kirkeby and P. A. Nelson, "Digital Filter Design for Inversion Problems in Sound Reproduction," J. Audio Eng. Soc. **47**(7/8), 583–595 (1999).

[4] Y. Kahana, P. A. Nelson, O. Kirkeby, and H. Hamada, "A multiple microphone recording technique for the generation of virtual acoustic images," J. Acoust. Soc. Am. **105**, 1503–1516 (1999).

[5] S. Yon and M. Fink, "Sound focusing in reverberating rooms and through walls: the time reversal approach," J. Acoust. Soc. Am. accepted in November 2002.

[6] M. Fink, "Time-reversed Acoustics," Phys. Today **50**(3), 34–40 (1997).

[7] M. Tanter, J.-L. Thomas, and M. Fink, "Time reversal and the Inverse filter," J. Acoust. Soc. Am. **108**, 223–234 (2000).

[8] C. Dorme and M. Fink, "Focusing in transmit-receive mode through inhomogeneous media: the time reversal matched filter approach," J. Acoust. Soc. Am. **98**, 1155–1162 (1995).

[9] M. Tanter, J.-F. Aubry, J. Gerber, J.-L. Thomas, and M. Fink, "Optimal focusing by spatio-temporal inverse filter, Part I: Basic principles," J. Acoust. Soc. Am. **101**, 37–47 (2001).

[10] P. Roux and M. Fink, "Time reversal in a waveguide: Study of the temporal and spatial focusing," J. Acoust. Soc. Am. **107**, 2418–2429 (2000).

[11] A. Derode, P. Roux, and M. Fink, "Robust acoustic time reversal with high-order multiple scattering," Phys. Rev. Lett. **75**(23), 4206–4209 (1995).

[12] J.-F. Aubry, M. Tanter, J. Gerber, J.-L. Thomas, and M. Fink, "Optimal focusing by spatio-temporal inverse filter. Part II. Experiments," J. Acoust. Soc. Am. **101**, 48–58 (2001).

[13] P. Blomgren, G. Papanicolaou, and H. Zhao, "Super-resolution in time reversal acoustics," J. Acoust. Soc. Am. **111**, 230–248 (2000).

[14] C. Prada and M. Fink, "Eigenmodes of the time reversal operator: a solution to selective focusing in multiple target media," Wave Motion **20**, 151–163 (1994).

[15] Acoustic attenuation D_T is defined as $D_T = L_1 - L_2$, where L_1 and L_2 are the mean sound levels measured in each room, for a white noise.